Chapter 9

Bioturbation by benthic stingrays alters the biogeomorphology of intertidal flats

Janne Nauta, Guido Leurs, Brian O. Nieuwenhuis, Donné R.A.H. Mathijssen, Han Olff, Tjeerd J. Bouma, Daphne van der Wal, Nadia Hijner, Aissa Regalla, Samuel Ledo Pontes, Laura L. Govers

Published in Ecosystems (2024)

Abstract

Fishing-down-marine-food-webs has resulted in alarming declines of various species worldwide. Benthic rays are one example of such overexploited species. On tidal flats, these rays are highly abundant and play an ecologically important role. They use tidal flats as refuge, feeding, and resting grounds, during which they bury into the sediment, which results in sediment bioturbation. Changes in bioturbation intensity following ray removal may affect the biogeomorphology of tidal flats with possible cascading effects on the macrozoobenthic community. However, it is poorly understood how these indirect effects could influence ecosystem function. We therefore studied the geomorphic impact of benthic rays (specifically the pearl whipray/stingray *Fontitrygon margaritella*) on the tropical tidal flats of the Bijagós Archipelago, Guinea-Bissau on a landscape-scale. We investigated 1) bioturbation rates by rays using drone- and ground-surveys, 2) the spatial distribution of ray pits on multiple tidal flats, 3) the impact of rays on sediment properties and macrozoobenthos by experimental exclusion (15 months). Benthic rays bioturbated 3.7±0.35% of the tidal flat's sediment surface per day over one single 24-hour period, which equals a complete top-sediment-surface turnover every 27 days. The spatial distribution of ray pits was affected by tidal flat geomorphology since pits decayed faster in areas exposed to strong hydrodynamic forces. Predator exclusion altered sediment properties, leading to changes in sedimentation (-17%) and erosion (-43%) rates. In addition, macrozoobenthic species composition changed, marked by an increase of Capitellidae worms and a greater biomass of Malacostraca over time. These changes indicated substantial effects of ray bioturbation on the biotic and geomorphic landscape of tidal flats. Overall, we conclude that changing abundances of benthic rays can have clear landscape-wide geomorphological effects on intertidal ecosystems. These indirect consequences of fisheries should be incorporated into integrative management plans to preserve tidal flats and connected ecosystems.

Introduction

Intertidal flats are prominent and productive geomorphic systems that provide valuable ecosystem services such as carbon storage, nutrient fluxes, coastal defense, primary and secondary productivity, fisheries enhancement and connection between marine and terrestrial ecosystems (Temmerman *et al.* 2013, Alongi 2014, 2018, van de Koppel *et al.* 2015, van der Zee *et al.* 2016). However, 16% of the world's intertidal flats have been lost due to anthropogenic pressures between 1984 and 2016 (Murray *et al.* 2019). Anthropogenic stressors, such as fishing, may disrupt natural equilibria with potential consequences for associated fauna and the ecological interaction networks they are part of (Pinnegar *et al.* 2000). Knowledge gaps on the interaction between threats (e.g., coastal fisheries), ecological functioning (e.g., food web structure, community composition) and the geomorphological development of intertidal flats (e.g., sedimentation, elevation) need to be addressed to improve effective management of these ecologically important areas, especially given the ongoing global loss of intertidal areas (Hill *et al.* 2021, Murray *et al.* 2022).

Fishing activities have caused dramatic declines in Chondrichthyes – shark, ray, and chimera populations on a global scale (Stevens *et al.* 2000, Baum *et al.* 2003, Baum and Myers 2004, Sherman *et al.* 2023), leading to an estimated 32% of 1,199 species currently being threatened with extinction (Dulvy *et al.* 2021). Although shark and ray species that use intertidal habitats are mostly affected by coastal mixed-species fisheries, they are also affected by industrial fisheries that operate on the edges of intertidal waters to catch animals that migrate into subtidal offshore areas (Dulvy *et al.* 2014, Leurs *et al.* 2021).

Most elasmobranchs are characterized by slow growth rates, late maturity, and low fecundity, and consequently highly vulnerable to direct human exploitation and bycatch mortality (Winemiller and Rose 1992, Jennings *et al.* 2001). Larger individuals are predicted to feed at higher trophic levels as size determines the dimensions of prey sizes that a predator can consume (Cohen *et al.* 1993). Larger predator overexploitation can control prey abundance through top-down processes (Bascompte *et al.* 2005), causing an increase in prey abundance (Myers *et al.* 2007, Ferretti *et al.* 2010, Sherman *et al.* 2020). However, these predator–prey dynamics need further investigation (Grubbs *et al.* 2016). On the other hand, when species of larger body size decline, fishing pressure may shift to smaller elasmobranchs such as benthic rays, known as 'fishing down the food web' (Pauly 1998). However, knowledge of the consequences of reduced ray numbers on ecosystem functioning is limited (Flowers *et al.* 2021).

Bioturbating benthic rays actively alter their habitats (i.e., habitat-modifiers) in search of food or resting grounds. To do so, these rays excavate and rework the sediment (hereafter referred to as 'ray pits') through a combination of protrusion of the jaws, water-jetting through the spiracles and movement of their pectoral fins (Freitas *et al.* 2019). These bioturbating activities can alter sediment erosion and composition (Takeuchi and Tamaki 2014) and create physical microhabitats that can benefit other species (Figure 9.1). For instance, ray pits can collect high amounts of organic matter, which benefits benthic detritus feeders (O'Shea *et al.* 2012). Bioturbation by rays thus alters geomorphological and ecological processes, which may ultimately affect the ecosystem functioning of intertidal flats (Lynn-Myrick and Flessa 1996, Needham *et al.* 2011, O'Shea *et al.* 2012). Moreover, these rays can be highly abundant in intertidal ecosystems and can play an important ecological role (Leurs *et al.* 2023a).

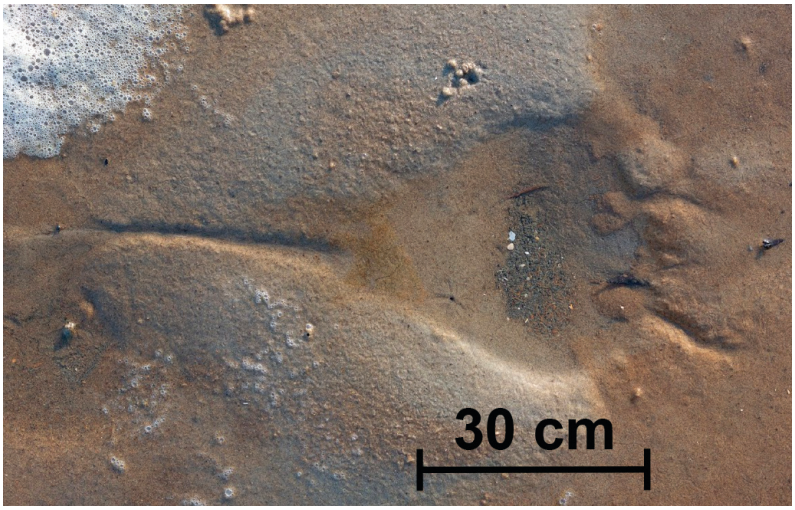

Figure 9.1 Excavation of the sediment created by benthic rays, called a 'ray pit'.

While the local-scale bioturbating effects of benthic rays are well studied (Grant 1983, O'Shea *et al.* 2012, Myrick and Flessa 2017), approaches to upscale these processes to a landscape scale are limited. In addition, experimental approaches to support ray bioturbation effects are inadequate (O'Shea 2012, Flowers *et al.* 2021). We studied the geomorphological impact of benthic rays using the tropical intertidal flats of the Bijagós Archipelago, Guinea-Bissau. Specifically, we quantified (1) the extent and intensity of benthic ray bioturbation at the intertidal flat landscape scale by conducting ground and drone surveys, (2) the spatial distribution and longevity of ray pits by looking at ray pit densities throughout the archipelago to test if the

abundance of ray pits could be influenced by intertidal flat morphology (e.g., ray pits erode faster under highly hydrodynamic conditions O'Shea *et al.* 2012), and (3) the effect of ray bioturbation on sediment properties and macrozoobenthos by means of a ray exclusion experiment. The study area was chosen to investigate the effects of benthic ray feeding behavior since intertidal flats are key habitats for benthic rays (Leurs *et al.* 2023a). In the Bijagós Archipelago, 896 to 2,685 rays were captured daily in 2020 if, respectively, 30% and 100% of the fishing fleet was active in 2020 (Leurs *et al. in prep.*). This is likely an underestimation of the actual catch as vessels from neighboring countries were unaccounted for (Leurs *et al. in prep.*). As global (including West African) coastal fisheries are currently increasing at an alarming rate (Dulvy *et al.* 2021, Leurs *et al.* 2021), studying the geomorphic effects of bioturbating rays now is relevant as changes in population densities of these fishery-targeted species may affect their ecosystem and the conservation status of benthic rays continues to deteriorate (Sherman *et al.* 2023).

Methods

Study site

The Bijagós Archipelagos (Guinea-Bissau) supports extensive protected intertidal flat areas where fisheries are restricted (Diop and Dossa 2011, Hill *et al.* 2021). These areas provide refuge for globally threatened elasmobranchs, including benthic rays (Diop and Dossa 2011, Campredon and Catry 2016). Therefore, this area is highly suitable for studying the landscape scale effects of these habitat-modifying species. As observed on intertidal flats, *Fontitrygon margaritella* is the most common species that could make these ray pits (Leurs *et al.* 2023). However, ruling out *Fontitrygon margarita* completely is impossible only from pit formations. We also know that the large majority (i.e., 140 out of 143, 97.9%) of *Fontitrygon* spp. sampled in the archipelago were *F. margaritella* from fish market sampling for stomach contents (Clements *et al.* 2022). Combined, these results indicate that the large majority of pits are created by *F. margaritella*. The archipelago islands consist of 88 islands and islets, which are the remaining peaks of the eroded and flooded sedimentary basin of the ancient delta of the Rio Grande and Rio Geba, off the coast of West Africa (Bird 2011), surrounded by mangroves and 760 km^2 of intertidal flats (Meijer *et al.* 2021). These islands are located at the southern end of the Senegalo-Mauritanien sedimentary basin, and sediments originate mostly from the Corubal and Geba rivers (Campredon and Catry 2016). These sediments are deposited and transported by complex hydrodynamic forces in a network of river channels. On the other hand, high annual rainfall (2200

mm) leads to high surface erosion rates (Bird 2011). The temperate southern Africa realm has a relatively stable tidal wetland (intertidal flats, tidal marsh and mangrove ecosystems) coastline (Murray *et al.* 2022). The Bijagós Archipelago has the highest tidal range of the West African coast, with spring tides reaching up to 4.5 m amplitude and strong currents up to 78 cm/s (Campredon and Catry 2016). These intertidal flats support up to 600,000 waders along the East-Atlantic Flyway (Salvig *et al.* 1994, Van Roomen *et al.* 2011, Campredon and Catry 2016), and because of the archipelago's extraordinary biodiversity, it was classified as a UNESCO Biosphere Reserve in 1996 and as a Ramsar site in 2014 (Ramsar Convention Secretariat 2014). Our research in the Bijagós Archipelagos occurred between October-December 2019 and February 2021 (Figure 9.2A).

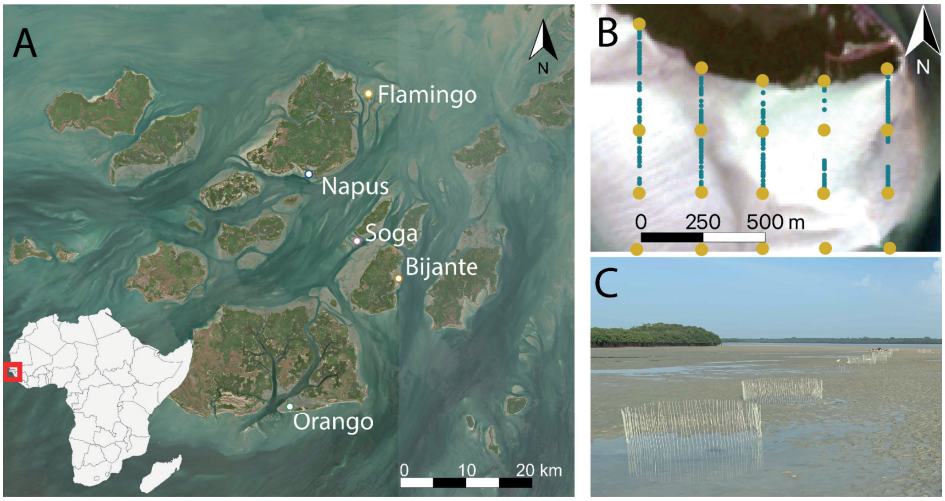

Figure 9.2 (A) Overview of the Bijagós Archipelago in Guinea-Bissau, West Africa (Sentinel-2 L2A, resolution: 10m, True color, 0% cloud cover, date: 2019/03/16). Napus, Orango, Bijante, Flamingo, and Soga are the intertidal flats. (B) An example of the transect survey at Napus (250 m between each transect) perpendicular to the mangrove fringe towards the subtidal area, where dots indicate ray pit abundances (blue) and sample locations of macrozoobenthos cores (yellow). (C) picture of the predator exclosure experimental setup.

Quantifying the extent of benthic ray bioturbation - drone survey

We mapped benthic-ray bioturbation pits of the Napus mudflat with a DJI Mavic 2 Pro drone (RGB) on the 15th and 16th of February 2021. For this, the high-resolution images (ground resolution = 0.5 cm/pixel) taken by the drone were stitched together using PIX4D. The mapped area covered an L-shape section of ~ 4.6 hectares, where the L-shape area was chosen to cover as much intertidal flats heterogeneity (e.g.,

sediment type and bathymetric elevation) as possible within the drone battery supply for one day. This image was overlaid with 64 squares of 16 m^2 each and positioned to capture as much spatial variation in ray pit abundance as possible. In every square, ray pits were manually annotated by visual observations in QGIS v.3.6.3 (QGIS Development Team 2018). To identify ray pits from other excavations (formed by other organisms or footprints), we color-marked all observed excavations in the field and consequently detected the differences in the size and shape of the excavations on drone images. Other organisms (i.e., other than stingrays) that may bioturbate the sediments of the Bijagós Archipelago are cownose rays, fiddler crabs and calianassid shrimps (Suchanek and Colin 1986, El-Hacen *et al.* 2019, Flowers *et al.* 2021). We identified the ray pits in this study from other excavations based on the size and shape of the pits that relate to the maximum disc width of the ray (~34 cm; Figure 9.1; Leurs *et al. in prep.*). Cownose ray pits (disc width up to 1 m; (Smith and Merriner 1985) are bigger than stingrays (Leurs *et al.* 2023a), and fiddler crabs and calianassid shrimps create smaller excavations (Suchanek and Colin 1986). For each of these squares, we compared the image of February 15th to that of February 16th and counted all newly formed ray pits. We analyzed the distribution of the newly formed ray pits according to normal (linear models; LM) and concentrated distribution (generalized linear models with Poisson or negative binomial distribution) and compared the Akaike Information Criteria for small sample sizes (AICs). To translate ray pit surface coverage into bioturbation rates, we used the amount of newly formed pits and the average pit volume measured in November 2019.

We performed all statistical analyses in R v.4.0.3 (R Core Team 2017). We validated all model assumptions by plotting (1) residuals versus fitted values to verify homogeneity, (2) QQ-plots of the residuals to test for normality and (3) residuals versus each explanatory variable to check for independence. In addition, Shapiro-Wilks's test ($p > 0.05$) and Bartlett's test ($p > 0.05$) were used to test for normality and homogeneity of variance, respectively. Surface bioturbation per day was log-transformed to meet model assumptions and analyzed by LM. Post-hoc comparisons were used to test for significant differences between the five intertidal flats (r-package 'emmeans'; (Lenth 2019). The relationship between pit counts on the 15th and 16th of February was fitted using a linear regression model.

Landscape-scale spatial ray pit distribution – observation surveys across the region

We quantified ray pit occurrence through transect counts for five sites across the archipelago (Figure 9.2B; Bijante = Bijante, Bubaque, N11° 15′ 24.3″ W15° 50′ 09.6″; Flamingo = Banco de Flamingo, Maio, Urok, N11° 33′ 18.1″ W15° 53′ 14.3″; Orango = Adonge, Orangozinho, N11° 02′ 10.2″ W16° 00′ 58.0″; Napus = Napus, Formosa, Urok, N11° 25′ 33.1″ W15° 58′ 59.3″; and Soga = Encromas, N11° 18′ 47.1″ W15° 54′ 01.1″). At each location, we sampled transects (n = 5 per location, but Soga n = 4, with 250 m distance between the transects) that covered the entire morphologic landscape of the intertidal flat and that was accessible by foot (from the edge of the subtidal to the mangrove edge). All ray pits within 1 meter of the transect line were measured along each transect. The length diameter, width diameter, depth radius, and water depth of each ray pit were measured. Additionally, the location of each ray pit was measured at 1cm precision with an RTK dGPS (Trimble R8, GNSS-receiver) connected to a local base station as a reference point. Small benthic rays in the Bijagós Archipelago are mostly represented by the most occurring stingray species, the pearl stingray (*Fontitrygon margaritella*; Leurs *et al.* 2023b). Hence, pit volume was calculated by treating the pits as a semi-ellipsoidal shape based on the body shape of the pearl stingray using equation 1 (O'Shea 2012, O'Shea *et al.* 2012, Myrick and Flessa 2017):

$$pit\ volume = (4/3\ \pi(Lr * Wr * Dr))/2$$

in which Lr is length radius (diameter/2), Wr is width radius (diameter/2) and Dr is depth radius.

The surface area covered with ray pits of the transects was log-transformed and consequently analyzed by LM and Tukey's posthoc comparisons to test for significant differences between the five intertidal flats (r-package 'emmeans'; Lenth, 2019).

Because of the spatial heterogeneity of the intertidal flats, we related the ray pit abundances to environmental parameters. To do so, we measured and/or obtained the parameters of the mudflat characteristics, macrozoobenthos, sediment properties and emergence time. First, we defined mudflat characteristics (i.e., distance to mangrove forests, gullies and subtidal waters) through QGIS based on the habitat classification of (Meijer *et al.* 2021); i.e., mangrove, mudflat and water depth). Habitat characteristics were manually verified by comparing the habitat classification of Meijer *et al.* (2021) to the satellite images (Sentinel-2 L2A, resolution: 10m, True color, 0% cloud cover, date: 2019/03/16) and adjusted if needed. For instance, based

on field observations, gullies that were known to remain inundated during low tide were added to the gully map. Second, to look at possible food sources of the rays, macrozoobenthos were sampled in a grid of 250 m spread across each intertidal flat (Figure 9.2B, *n* = 20 per intertidal flat) with a PVC core of ⌀ 15 cm to a depth of ~25 cm. Each sample was sieved over a 1 mm round mesh (Compton *et al.* 2013). After sample collection, all macrozoobenthos samples were stored in 10% formaldehyde and identified to species level in the laboratory. After identification, species were dried for 24 h at 60°C and incinerated for 4 hours at 550°C to determine Ash Free Dry Weight (AFDW). Third, sediment samples were taken in the same 250 m grid as the macrozoobenthos samples. To analyze sediment composition, we sampled the top-1 and top-5 cm of the sediment surface with a small core of ⌀ 2.5 cm and determined the organic matter content of the soil, median grain size D50 (μm) and silt% (grain size <63 μm). For the calculation of organic matter content, the AFDW of sediment samples was determined, and the percentage weight loss on ignition (LOI_{wt}%) was calculated. To measure median grain size and silt%, sediment samples were freeze-dried (-550 C, 48 h), sieved over 1-mm mesh and analyzed with the Malvern Mastersizer 2000 (Malvern Instruments, Worcestershire, United Kingdom, serial number 34403/139, model APA 2000 with Hydro G 2000 introduction unit and Autosampler 2000). Last, emergence time was derived from the results of (Granadeiro *et al.* 2021) that estimated exposure with Sentinel-2 satellite imagery.

To correlate the environmental parameters to the ray pit abundances, we performed ordinary kriging to interpolate any missing data points for median grain size D50, silt% and macrozoobenthos AFDW based on the 250 m grid samples (*n* = 20 samples per intertidal flat with a sampling and interpolation coverage of 0.5-0.75 km^2; r-package: 'automap'; Hiemstra, 2022) in R (R Core Team 2020). The function 'autoKrige' fits a variogram model to the given data set and returns the results of the interpolation: prediction, variance and standard deviation. The environmental parameters of ray pit abundance were modeled with a generalized additive model (GAM) with smooth splines to allow fitting any non-linear pattern (r-package 'mgcv'; Wood 2017), where intertidal flats were modeled as a random factor. Ray pit abundance was zero-inflated and tested with r-package 'DHARMa' (Hartig 2023). We tested if the smooth terms were necessary by running the model with and without smooth terms for each predictor separately. The lowest AIC was reached by including smooth terms on all the predictors, except sediment median grain size D50, and the significance of smoothers was tested via an adapted Wald test (Wood 2017). The GAM's smoothers were estimated through restricted maximum likelihood to prevent overfitting.

Residual spatial autocorrelation was inspected by fitting a GAM with a tensor product of the coordinates to the residuals of the original GAM (Wood 2017). GAM model selection was performed by ranking all possible subsets of the full GAM based on AICc (r-package 'MuMin'; (Bartón 2022)). The optimal subset approach was used because it performs best when comparing models that contain correlating measurements. Adjusted R-squared values were used to assess overall model performance.

To test for the sensitivity of the ray pits longevity to exposure, we measured the longevity of artificial pits (*n*=20, starting pit size was 25x24x4 [LxWxD]) in two locations with expected high and low exposure to hydrodynamic forces. High exposure locations were situated exposed to the incoming tide at 100-300 m to the subtidal waters, whereas low exposure locations were situated at the mangrove edge, sheltered by the intertidal flat at 300-500 m to the subtidal waters. Measurements were taken for 84 h with a 12-36 h interval depending on accessibility.

Although we expected differences in exposure to hydrodynamic forces, the locations were chosen based on a comparable elevation, with, on average, a relative difference of +8.9 cm at the mangrove edge compared to the exposed location, measured at 1-cm precision with an RTK dGPS (Trimble R8, GNSS-receiver) connected to the local base station as a reference point. Ray pit longevity was analyzed with linear regression models.

Ray bioturbation effects on sediment and macrozoobenthos – exclusion experiment

To test the consequences of benthic ray absence on sediment properties and macrozoobenthos, we experimentally excluded predators (e.g., rays and birds) with a 15-month exclosure experiment. We installed 30 circular experimental plots (diameter of 2 m) in October 2019 (Figure 9.2C). We deployed the following experiment treatments: *i)* predator exclosure (exclosure, *n* = 12), *ii)* effect of exclosure (one-sided, open exclosure; *n* = 6), and *iii)* no exclusion (control; *n* = 12). Predators were excluded with barriers made of glass-fiber sticks (1 x 0.003 m, length x diameter) inserted halfway (50 cm) into the sediment at a 5 cm interval. For the open exclosure, we constructed plots with only half of the circle (⌀ 2 m) covered by glass-fiber sticks to test for the geomorphic effects of the exclosure method on sediment properties. These open exclosures were installed with the opening to each of the cardinal directions (*n* = 3 per cardinal direction, north, east, south and west; total *n* = 12). The plots were spaced 3.5m apart in a randomized block design. The contours of the control plots were

marked by four sticks, which had no further exclosure function. After counting ray pits in the experimental plots, we could confirm that the exclosures were effective for benthic rays since 0 ± 0% (mean ± s.e.) of the exclosures contained ray pits, compared to 48 ± 6% and 33±6% in the open exclosures and control, respectively (Appendix 9.1). However, the exclosures also seemed to be effective in excluding wading birds since we observed bird tracks in 5 ± 0 % of the exclosures, compared to 42±6% and 45±6% in the open exclosure and control. For the entire duration of the experiment, plots were inspected and maintained for fouling, scouring, and missing sticks once every two months on average. After 15 months of deployment of the exclosures, we sampled macrozoobenthos and sediment properties. The macrozoobenthos were sampled with a PVC corer of Ø 15 cm to a depth of ~25 cm, sieved over a 1 mm round mesh (Compton *et al.* 2013), fixated in 10% formaldehyde and identified to species level in the laboratory. After identification, we measured species abundance and biomass. Species were dried for 24 h at 60°C and incinerated for 4 hours at 550°C to determine Ash Free Dry Weight (AFDW). Sediment properties were sampled with a small core of Ø 2.5 cm (the top-1 and top-5 cm of the sediment surface) and analyzed for organic matter content of the soil, median grain size D50 (μm) and silt% (grain size <63 μm). To calculate organic matter content (percentage weight loss on ignition (LOI $_{wt}$%)), sediment samples were dried for 24 h at 60°C and incinerated for 4 hours at 550°C. To measure median grain size and silt%, sediment samples were freeze-dried (-550 C, 48 hours), sieved over 1-mm mesh and analyzed with the Malvern Mastersizer 2000 (Malvern Instruments, Worcestershire, United Kingdom, serial number 34403/139, model APA 2000 with Hydro G 2000 introduction unit and Autosampler 2000). In addition, the effect of ray exclusion on sediment dynamics was investigated with sediment erosion pins (Nolte *et al.* 2013). Upon installation in 2019, each plot was equipped with two sediment pins that consisted of a thin one-meter-long metal rod anchored ~85 cm into the sediment, with a loosely fitting metal ring surrounding it at the sediment surface. This allowed us to track maximum erosion, sediment accretion and net change of the sediment's surface elevation over the experimental period of 15 months.

The impact of predatory exclusion on macrozoobenthos was visualized using Non-Metric Multidimensional Scaling (NMDS) (Kruskal and Wish 1978) on Bray-Curtis dissimilarity indices (Clarke and Green 1988) using r-package 'vegan' (Oksanen 2019). For this analysis, rare species, defined as species with less than two total occurrences, were excluded to prevent them from appearing too influential in the graphical representation of the ordination (Poos and Jackson 2011). Differences

between the treatments were tested with permutational multivariate analysis of variance (PERMANOVA, 999 permutations), incorporating experimental blocks as a random intercept. To test for the effect of predator exclusion on abiotic parameters, we used linear mixed-effect models (LMM) with 'block' as a random factor. Post-hoc comparisons were used to test for significant differences between the effect of predator exclosure, open exclosure and control (r-package 'emmeans'; Lenth 2019).

Results

Benthic ray sediment bioturbation

To examine benthic bioturbation rates, we surveyed newly formed ray pits and volumes on two consecutive days at the intertidal flat Napus. The distribution of ray pits varied between 0 and 2 newly formed ray pits m^{-2}. The distribution of these pits related to the environmental predictors (distance to creek, distance to mangroves and elevation) was best described according to concentrated foraging patterns (negative binomial distribution) versus random distribution (normal distribution; Appendix 9.2). To estimate the surface that was bioturbated by the excavation of these pits, we used the average pit volume of 1475.87 cm3 (n = 440 at Napus 2019) to calculate the bioturbation rates based on the number of newly formed ray pits on one single 24-hour period in February 2021. To estimate the surface that was bioturbated by the excavation of these pits, we used the average pit volume of 1475.87 cm^3 (*n* = 440 at Napus 2019) to calculate the bioturbation rates based on the number of newly formed ray pits over one single 24-hour period in February 2021. We found that ray pit excavation bioturbated the sediment surface with 3.7±0.4% per day (mean±SE) and up to 14.3% per day. This equals a volume of, on average, 765.3 ± 73.0 $cm^3m^{-2}day^{-1}$ measured over one single 24-hour period and is equivalent to a turnover rate of 27 days. The total surface covered with ray pits on the intertidal flats of Napus on the 15th of February was 4.97 ± 0.68% (mean ± s.e.; Figure 9.3).

Consequently, we used the relationship between the total amount of pits and newly formed pits measured in 2021 to estimate the bioturbation rates on all five intertidal flats measured in 2019. The relation between the total amount of ray pits on February 15th and the newly formed pits on February 16th could be described according to linear regression*: y* = 5.58 + 0.274*x* (Figure 4b, *R2* = 0.52). Implementation of this linear regression on the measurements of November 2019 (start of the experiment, described in section 3.2 below) implied that bioturbation rates at that particular moment ranged between 0.14±0.04 and 0.44±0.10% (mean±SE, Figure 4c, 1-way

ANOVA, $F_{4,19} = 7.1314$, $p < 0.001$). These bioturbation rates in February 2021 were 8.4 times higher at Napus compared to November 2019, and therefore, it is likely that bioturbation rates vary daily, seasonally and/or yearly.

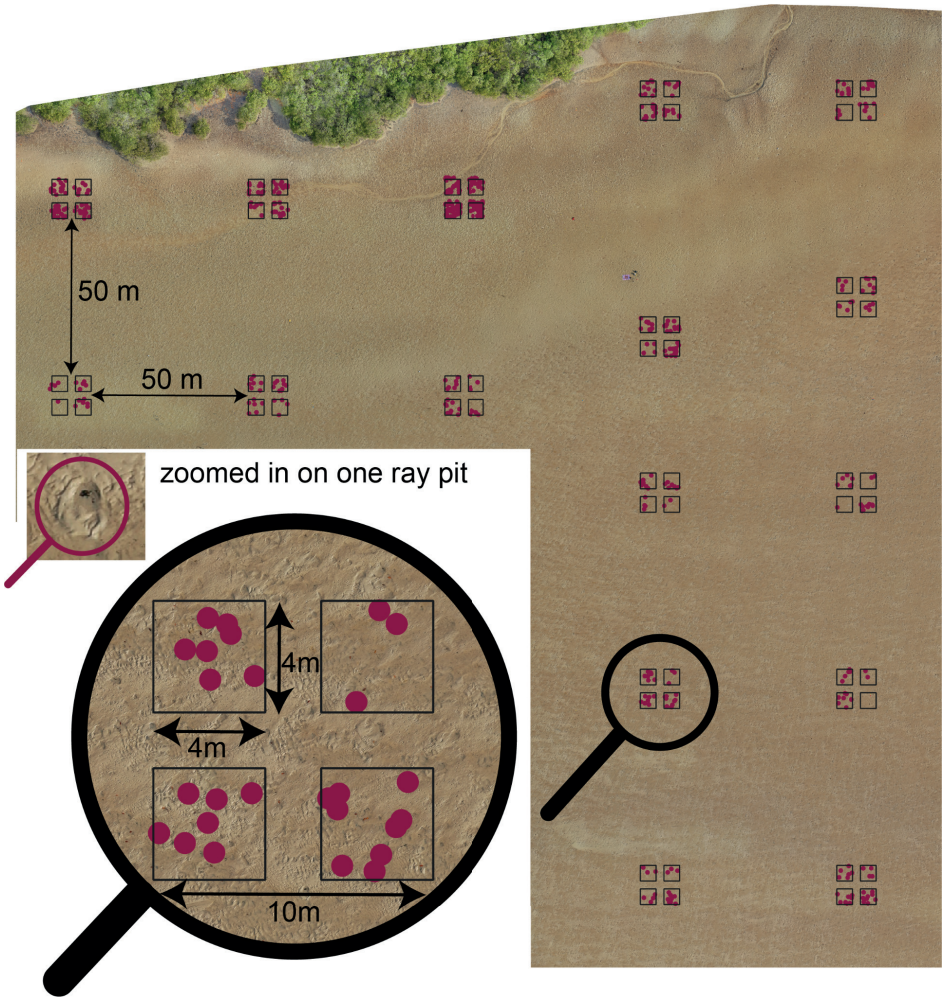

Figure 9.3 Annotations of new ray pits on the tidal flat Napus on February 16th, 2021. An example of one zoomed-in ray pit is shown (insert, top-left). High bioturbation of 3.70 ± 0.35% of the surface area per day was observed and measured over one 24-hour period (mean ± SE). This bioturbation had a volume of 765.31 ± 72.97 cm3 m-2 day-1 (mean ± SE).

Benthic ray pit abundance, spatial distribution and longevity

We determined if the abundance of ray pits could be influenced by the intertidal flat morphology. For example, ray pits erode faster under highly hydrodynamic conditions (O'Shea *et al.* 2012). We counted the number of ray pits at five intertidal flats through a field survey in November 2019. We found that the total excavated surface area significantly differed among intertidal flats and ranged between 0.39 ± 0.50 and 1.30 ± 1.64% of the total intertidal flat surface area (mean ± s.e.) (Figure 4a, one-way ANOVA, $F_{2,19}$ = 5.566, p = <0.001). In addition, there was a great level of ray pit spatial heterogeneity within the intertidal flats. To explain the spatial distribution of ray pits within the intertidal flat landscape, we investigated the relation of pit abundance to environmental parameters (Table 9.1). The distribution of these ray pits could be predicted (deviance explained 35.3%) based on sediment characteristics: median grain size D50, silt%, organic matter content, distance to the subtidal and emergence time (Table 9.1).

To test for a relationship between ray pit abundance and morphology, we measured the longevity of hand-made ray pits at two locations with differing exposure but comparable elevation (on average +8.9 cm at the mangrove edge compared to the exposed location). We found a 3.5 times faster pit volume decay rate at the exposed location with a coefficient of -2.87 (R^2 = 0.88), compared to -0.81 (R^2 = 0.46) at a location sheltered by the intertidal flat itself (mangrove edge; Appendix 9.3). This means that, after 24 hours, only 17.2% of ray pit volume remained in exposed areas, in contrast to 74.0% of the original pit volume remaining in sheltered areas.

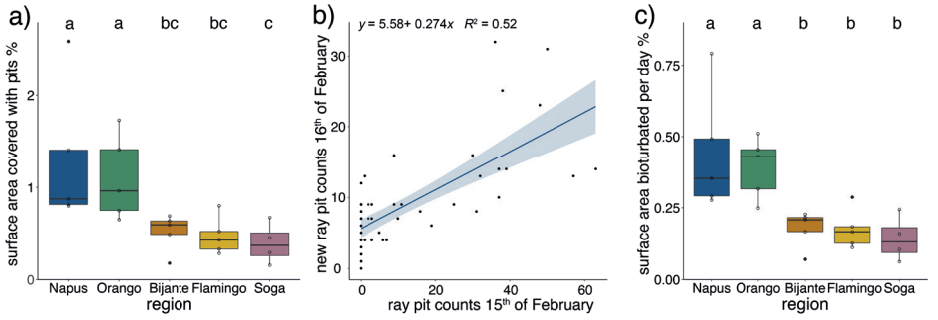

Figure 9.4 (A) High tidal flat surface area covered with ray pits in percentage, based on the observational survey with transects (n = 5 per tidal flat, Soga n = 4) in November 2019. Letters indicate significant differences tested with Tukey's posthoc; **(B)** relation between ray pit counts on the 15th of February and newly formed pit counts on the 16th of February 2021. The surface of the tidal flats bioturbated per day was calculated using linear regression and the ray pit abundances of Figure 9.3, resulting in **(C)** total surface area percentage bioturbated per day per tidal flat in November 2019 (n = 5 per tidal flat, Soga n = 4).

Predator exclusion effects on sediments and macrozoobenthos

The exclusion of predators such as rays and shorebirds created muddier and more stabilized sediments, a higher abundance of Capitellidae worms, and a greater biomass of Malacostraca over time (15 months). Silt and organic matter content were 20% (Tukey, $p<0.01$) and 10% (Tukey, $p<0.001$) higher, respectively, in the top-5 sediment layer of the exclosures than in the control plots in February 2021 (Table 9.2), while there were no differences in sediment properties at the start of the experiment (November 2019, Appendix 9.1). In addition, the exclosures showed -17% sedimentation (Tukey, $p<0.01$) and -43% erosion (Tukey, $p<0.0001$) after 15 months (Table 9.2), indicating higher sediment stability. Furthermore, we found no effects of the open exclosures on sediment properties (e.g., median grain size, silt%, organic matter content, erosion, accretion) as the open exclosures yielded results similar to the controls (Table 9.2). We can therefore safely assume that the effects of the exclosures on sediment properties are the result of predator exclusion and not an effect of the exclosure structures themselves. Moreover, predator exclusion altered the macrozoobenthic community composition (after 15 months) based on species biomass (Figure 5; PERMANOVA, n = 999, $F = 6.38$, $p < 0.001$) and species abundance (Appendix 9.4; PERMANOVA, n = 999, $F = 3.52$, $p < 0.01$). In February 2021, this difference could partly be explained by a 1.8 times higher abundance of polychaete worms of the Capitellidae family and a 4.0 times higher biomass of Malacostraca in the exclosure compared to control, while a 0.6 times lower abundance of both Pilargidae and Nereididae was observed (Appendix 9.5, 9.6). The biomass of the bivalves *Tagellus adonsonii* and *Senilia senilis* in the exclosure are responsible for outliers at both the start (three times higher compared to control in November 2019) and end (25 times higher compared to control in February 2021) (Appendix 9.5, 9.6). .

Table 9.1 Significance of smoothers and model summary statistics of four best model subsets ranked by lowest AICs of the GAM predicting ray pit abundance. The predictors are distance to subtidal water, emergence time, sediment median grain size D50 in µm, sediment silt%, sediment organic matter content (OM), and region of the tidal flats as a random effect. If the environmental parameter is included in the model, it shows a significance level. Therefore, empty cells indicate that the specific parameter is not included in that model. The ray pit abundance data includes all five flats, with the flat as a random factor. ***<0.001, **<0.01, ns means not significant.

rank	distance subtidal	emergence time	sediment OM	region as random effect	silt%	grainsize (D50)	distance gully	df	AICc	weight	deviance explained
1	***	*	***		***	***		30	2071.1	0.298	35.3
2	***	*	***	n.s.	***	***		30	2071.1	0.297	35.1
4	***	*	***	n.s.	***	***	n.s.	37	2071.9	0.203	35.8
5	***	*	***		***	***	n.s.	37	2071.9	0.203	35.9

At the start of the experiment, the macrozoobenthic communities did not differ between the exclosure and control for both species' biomass and abundance (Appendix 9.7, 9.8; PERMANOVA, n = 999, abundance: $F = 0.53$, $p = 0.809$, biomass: $F = 0.76$, $p = 0.674$)

Table 9.2 The effects of predator exclosure on sediment properties, accretion and erosion levels compared to the open exclosure and control treatments. Letters indicate significant differences tested with Tukey's post-hoc.

			predator exclosure	open exclosure	control
sediment layer	variable	unit	mean (SE)	mean (SE)	mean (SE)
top 1 cm	median grain size (D50)	µm	217.87 [a] (1.93)	223.12 [ab] (4.40)	231.93 [b] (4.69)
top 1 cm	silt <63 µm	%	3.81 [a] (0.19)	3.25 [b] (0.20)	2.81 [b] (0.17)
top 1 cm	organic matter (Loss Of Ignition)	%	1.01 [a] (0.02)	0.95 [ab] (0.03)	0.90 [b] (0.03)
top 5 cm	median grain size (D50)	µm	221.43 [a] (3.18)	221.14 [a] (4.62)	232.86 [a] (3.91)
top 5 cm	silt <63 µm	%	2.97 [a] (0.10)	2.70 [ab] (0.13)	2.45 [b] (0.13)
top 5 cm	organic matter (Loss Of Ignition)	%	0.88 [a] (0.02)	0.81 [b] (0.02)	0.80 [b] (0.03)
na	ray pits	fraction	0.00 [a] (0.00)	0.48 [b] (0.06)	0.33 [b] (0.06)
na	accretion	cm	5.74 [a] (0.28)	6.39 [ab] (0.25)	6.72 [b] (0.23)
na	erosion	cm	4.72 [a] (0.32)	6.35 [b] (0.35)	6.75 [b] (0.26)
na	net surface change	cm	1.03 [a] (0.32)	0.04 [a] (0.44)	-0.02 [a] (0.38)

Discussion

Rays are sensitive to overfishing and rapidly disappearing from intertidal flat ecosystems (Dulvy *et al.* 2021). Rays can be important in determining the community structure and morphology of intertidal flats through natural physical disturbance by bioturbating the sediment. Bioturbation is a key factor in sediment transport, porosity and permeability (Thistle 1981, Thrush *et al.* 1991, Meysman *et al.* 2006). However, the ecological role of these foundation species in intertidal ecosystems is still poorly understood. We therefore linked ray bioturbation – and the absence of this behavior – to landscape-scale intertidal flat geomorphology in a relatively less-exploited (i.e., high abundance of benthic rays) tropical intertidal system (Leurs *et al.* 2023b).

These ray abundances are estimated based on small-scale fisheries ray catches by Leurs *et al.* (*in prep.)* using satellite-based vessel counts and a short-term observer program that estimated that 896 to 2,685 rays were captured daily in 2020 in the Bijagós Archipelago (Leurs *et al. in prep.*). We found that benthic rays affect intertidal flat sediment dynamics by digging excavations and bioturbating 3.7% of the total sediment surface per day over one single 24-hour period. This implies that the entire sediment surface area is reworked by rays every 27 days. These bioturbation rates varied substantially on a landscape level, among years, intertidal flats and within one intertidal flat landscape. Furthermore, the absence of natural physical disturbance by rays, simulated by a long-term exclosure experiment, increased sediment stability (reduced erosion and accretion) and increased silt% and organic matter content in the top sediment layer.

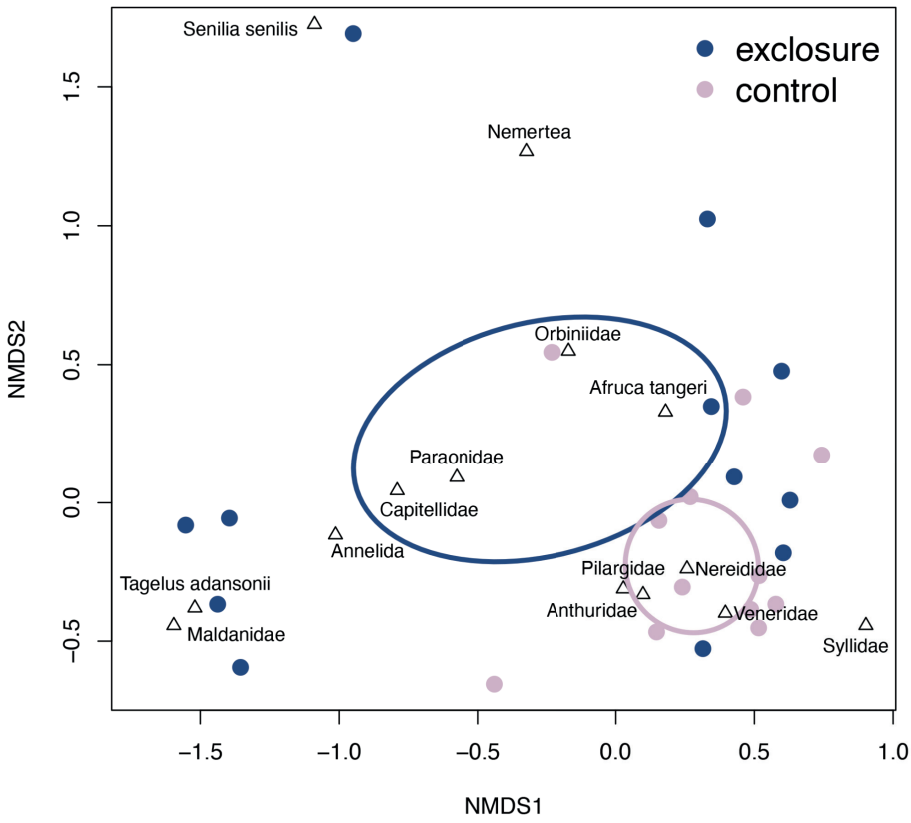

Figure 9.5 Ordination of taxa composition based on species biomass (ash-free dry weight m^{-2}) in the predator exclosures compared to the control plots without any exclusion visualized with Non-Metric Multidimensional Scaling (nMDS) on Bray-Curtis dissimilarity indices and reliable ordination (stress value < 0.2). Ellipses indicate the precision of the estimated centroid (SE) with a 95% confidence interval.

This indicates the importance of natural physical disturbance by benthic rays on intertidal flat biogeomorphology. In addition, the long-term (15 months) exclosure experiment changed the macrozoobenthos community composition by a higher abundance of Capitellidae worms and a greater biomass of Malacostraca over time. Although we were unable to separately exclude rays or wading birds in the predator exclosure experiment, we can safely assume that the bioturbation effects are due to ray excavation, given that birds feed without bioturbating the sediment surface (Lourenço *et al.* 2017, 2018). Furthermore, previous research found that bioturbation by benthic rays can change the sediment biogeochemistry of sandflats by rapid remineralization of organic matter, slowed flushing near the ray pits and increased reactive carbon supply (D'Andrea *et al.* 2002). Hence, overexploitation of benthic rays may alter the ecosystem functioning of threatened intertidal flat seascapes.

Benthic rays can substantially alter intertidal flat sediment turnover by sediment bioturbation, and the magnitude of sediment displacement rates (mean of 765.31 $cm^3m^{-2}day^{-1}$) found in this study further underlines the importance of these ray-induced processes for intertidal flat morphology. The sediment bioturbation rates that we found (on average 3.7% and a maximum of 14.3% day^{-1} over one single 24-hour period) were higher than the previously reported stingray bioturbation rates e.g., 2.42% in seven days in Ningaloo reef in Australia (Grant 1983, Sherman *et al.* 1983, O'Shea *et al.* 2012) or 1.4% day^{-1} on intertidal sand flats of the North Island of New Zealand (Thrush *et al.* 1991). Our sediment displacement rates fall within the range of previously reported studies (Lynn-Myrick and Flessa 1996, O'Shea *et al.* 2012). However, previous research elaborates that benthic ray bioturbation has the most relevance at the micro- and mesoscale (O'Shea *et al.* 2012) or studied at smaller tidal areas (0.11 km^2 and only one intertidal flat; (Takeuchi and Tamaki 2014), we demonstrated that ray bioturbation plays a significant role on a landscape-scale throughout the region (study area of 0.5-0.75 km^2 per intertidal flat * five intertidal flats). This is comparable to the landscape scale at which flamingos and fiddler crabs create essential microhabitats in Mauritanian intertidal flats (El-Hacen *et al.* 2019). Bioturbation rates may vary across studies because of differences in local ray densities, species-specific bioturbating behavior and body size, or the visibility of the pit on the intertidal flat surface (Flowers *et al.* 2021).

Benthic ray bioturbation rates are influenced by the ray densities (biotic) and pit longevity (abiotic). First, ray densities are affected by the season or year (Leurs *et al.* 2023b). Leurs *et al.* (2023b) found that seasonal differences in species richness and species composition of elasmobranch are caused by changes in stingray (the pearl

whipray *Fontitrygon margaritella)* abundances, and that species composition differed between non-protected and protected areas when seasonality is taken into account. In addition, we found 8.4 times higher bioturbation rates in February 2021 compared to November 2019, and (Thrush *et al.* 1991) observed a prevalence of rays during summer (November to March in New Zealand). Likewise, industrial fishing activities show the highest mean catches of benthic rays in April-June along the coast of Guinea-Bissau (Leurs *et al.* 2021). Second, ray densities can vary among intertidal flats within the region. For example, our study shows a bioturbation rate ranging from 0.2% to 14.3% per day. Third, ray spatial distribution can differ within the intertidal flat landscape because of spatial heterogeneity such as food availability (Hines *et al.* 1997, Ajemian and Powers 2012), predator risk (Strong *et al.* 1990, Stephens *et al.* 2007) and the risk of entrapment in areas that will fall dry with the receding tides (Brinton and Curran 2017, Leurs *et al.* 2023a). On the other hand, we found that exposure to hydrodynamic forces of the intertidal flat played an important role in the longevity of the ray pits (abiotic) as a result of more exposure to hydrodynamic forces and less cohesive soil (Wang *et al.* 2019). Our study showed that only 17.2% of pit volume was left after 24 h in exposed areas compared to 74.0% in an area sheltered by the intertidal flat. Thus, shorter longevity (<1 day) of ray pits in highly exposed areas might give an underestimation of benthic ray bioturbation. In summary, the interplay of biotic and abiotic factors determines the measured intertidal flats' bioturbation rates by benthic rays and, in addition to bioturbation, benthic rays further impact the environment by foraging on macrozoobenthos (Lynn-Myrick and Flessa 1996, O'Shea *et al.* 2013, Lim *et al.* 2019).

We found that predator exclusion significantly changed the macrozoobenthic community, specifically higher Capitellidae abundances and malacostraca biomass. However, these results should be interpreted with caution since we were not able to exclude rays only, but also excluded shorebirds. Previous research observed no impact and suggested ineffective ray exclusion (O'Shea 2012) or used a limited number (n=2) of replicates and reported scouring (VanBlaricom 1982). In addition, (Thrush *et al.* 1994) found fewer bivalve recruits in predator (ray + bird) exclosure but could not distinguish ray and bird effects due to seasonality. In the Bijagós, the most abundant meso-predatory ray, *F. margaritella*, shows a generalist's diet with relative contributions of 30%–35% by crustaceans and 17%–25% by polychaetes (Clements *et al.* 2022). These dietary preferences match the observed community changes in the exclosure experiment. Overall, a ray's turbulent foraging strategy may especially affect long-lived, sedentary species (O'Shea 2012, Jacobsen and Bennett 2013, Freitas *et al.* 2019). As the standing macrozoobenthic biomass in the Bijagós Archipelago is,

on average, low compared to other intertidal flat ecosystems (Lourenço *et al.* 2018, Meijer *et al.* 2021), it is likely that the observed high ray pit abundances (up to a mean of 1.30% per total surface area), combined with low macrozoobenthic biomass, indicate a high foraging pressure by benthic rays and other (meso-) predators such as shorebirds. Shorebirds are predators with small trophic niches that feed without bioturbating the mudflat (Catry *et al.* 2016, Lourenço *et al.* 2017, 2018). Shorebirds in the Bijagós Archipelago forage on fiddler crabs, polychaetes (*Nereis*, *Glycera* and *Marphysa*) and the bivalve *Dosinia isocardia* (Lourenço *et al.* 2017) but consume, in general, a high diversity of prey (Correia *et al.* 2023). Shorebirds are major players in intertidal food webs because they occupy a central niche (Mathot *et al.* 2018). Recent findings suggest that (meso)predators such as sharks and rays (i.e., high-tide predators in the intertidal) occupy a similar central niche as shorebirds in intertidal food webs and should therefore be considered in intertidal ecology (Leurs *et al.* 2023a). High foraging pressure of rays may even cause a food conflict with shorebirds foraging on the same intertidal flats and competing for the same scarce prey species (Lourenço *et al.* 2017, 2018), and affect intertidal, subtidal and terrestrial food webs through shorebird migration along the East Atlantic Flyway.

The importance of ray bioturbation to the ecosystem depends on the magnitude of other environmental and biotic factors that can disturb the sediment, such as tidal waves and currents, extreme weather events, and the impact of other bioturbating organisms. High forces of water movement can displace large volumes of sediments that may overrule the impact of ray bioturbation. For example, (D'Andrea *et al.* 2002) described that ray pits are short-term depositional centers for reactive organic matter that alter the sediment structure for 1 – 4 days. This study is limited by the information we collected regarding sediment displacement rates of intertidal flats controlled by water movement. However, it is known that the Bijagós Archipelago is a relatively stable intertidal ecosystem with low changes in the intertidal flat area compared to other intertidal areas of the world (Murray *et al.* 2019, 2022). In addition, West Africa has relatively low chances of extreme weather events such as cyclones because most Atlantic tropical cyclones are developed in the West African region, moving from east to west (Goldenberg and Shapiro 1996, Hopsch *et al.* 2007). Moreover, we observed a low presence of burrows from other bioturbation species, such as calianassid shrimps (Calianassidae), that can overturn sediments at an estimated peak rate of 0.47 - 0.56 m^{-3} m^{-2} $year^{-1}$ (Suchanek and Colin 1986, Myrick and Flessa 2017). Although this study has limitations, our results show that short-term ray bioturbation effects on the sediment are maintained at a landscape scale and may co-shape intertidal flat morphology and abiotic settings.

Our study showed that complex biogeomorphic interactions, in which organisms influence sedimentary processes, underpin intertidal flats ecosystem functioning. The protection of bioturbating species should be better integrated into coastal management plans for intertidal flat conservation, given that the natural physical disturbance by rays plays an important role in sediment turn-over rates and structuring of the macrozoobenthic community on landscape scales. Since intertidal flats are highly connected ecosystems globally, the need for protection, both locally and internationally, on a highly interconnected habitat level is further emphasized. For example, fishing activities in adjacent marine habitats affect the ray population in intertidal ecosystems (Dulvy *et al.* 2021, Leurs *et al.* 2021). Hence, disruption of intertidal flats' high ecological value can affect other connected ecosystems and vice versa.

Conclusion

We conclude that benthic rays affect landscape-scale sediment processes and community structure through bioturbation and, thus, intertidal flat biogeomorphology. This study highlights that local ecological processes (ray bioturbation) play a significant role at the landscape scale. Neither marine nor terrestrial protected areas are developed to prioritize intertidal flat conservation, and intertidal flat conservation generally focuses on total coverage instead of targeting valuable ecosystem services or species (Dhanjal-Adams *et al.* 2016, Hill *et al.* 2021). Therefore, coastal management strategies to protect intertidal ecosystems may benefit from an integral and connective approach linking the subtidal offshore (industrial) fishing activities to intertidal ecosystem functioning. Changes in species abundance as a result of offshore fishing activities that target highly mobile species, such as benthic rays that migrate in both subtidal and intertidal waters, can affect sedimentary processes in the intertidal area. This has associated consequences for species composition, for example, the dominance of species due to reduced physical disturbance.